

*Hubble Space Telescope* Observations of the Planetary Nebula K 648  
in the Globular Cluster M15<sup>1</sup>

David R. Alves, Howard E. Bond, and Mario Livio

Space Telescope Science Institute, 3700 San Martin Dr., Baltimore, MD 21218

Emails: `alves`, `bond`, `mlivio@stsci.edu`

arXiv:astro-ph/0007190v1 13 Jul 2000

---

<sup>1</sup>Based on observations with the NASA/ESA *Hubble Space Telescope*, obtained at the Space Telescope Science Institute, which is operated by AURA, Inc., under NASA contract NAS5-26555.

## ABSTRACT

We have obtained observations of the planetary nebula K 648 in the Galactic globular cluster M15 with the *Hubble Space Telescope's* WFPC2 camera, covering an interval of 7 days. The frames provide both time-sampled broad-band photometry of the central star and high-resolution images of the nebula in the light of  $H\alpha$ , [O III], and [N II].

In the deep narrow-band images, K 648 is a fairly typical double-shelled elliptical, but with a bright arc at one end of the major axis that is especially prominent in [N II]; this feature is probably a collection of FLIERs (fast low-ionization emission regions). The nebula is surrounded by a faint, smooth elliptical halo, which appears undisturbed by any interaction with the interstellar medium.

Adopting  $T_{\text{eff}} = 40,000 \pm 3,000$  K based upon published spectral-line analyses, and employing our new broad-band optical flux data along with the known cluster distance, we find  $\log L/L_{\odot} = 3.78 \pm 0.08$  for the K 648 central star. Theoretical post-asymptotic-giant-branch evolutionary tracks imply a mass of  $0.60 \pm 0.02 M_{\odot}$  for this luminosity, which is significantly higher than the mean mass of white dwarfs in globular clusters and the halo field ( $0.50 \pm 0.02 M_{\odot}$ ). The K 648 central star exhibits no significant photometric variability in our data; thus we find no direct evidence of a close binary companion. We suggest that the progenitor of K 648 experienced mass augmentation in a close-binary merger, allowing it to evolve to a remnant of higher mass than those of the single stars in the cluster.

*Subject headings:* planetary nebulae: general — planetary nebulae: individual (K 648, Ps 1) — globular clusters: general — globular clusters: individual (M15) — binaries: close

## 1. Introduction

A small number of planetary nebulae (PNe) are associated with the Galactic halo, on the basis of their kinematics, Galactic locations, chemical compositions, and/or memberships in globular clusters. These halo PNe (called Type IV by Peimbert 1978) are of particular interest because they arise from the low-mass and low-metallicity extremes among PN progenitor stars, and are thus important objects for testing our understanding of PN formation.

Eight halo PNe are known in the field (see Howard, Henry, & McCartney 1997 and references therein). Four additional PNe are known in Galactic globular clusters (GCs), including the subject of this paper and the prototype of the class, K 648 in the cluster M15 (NGC 7078). First cataloged as a star by Küstner (1921), K 648 was shown to be a PN by Pease (1928). During the ensuing six decades K 648 remained unique, but recently PNe have also been found in the GCs M22 (Gillett et al. 1989) and Pal 6 and NGC 6441 (Jacoby et al. 1997).

It is currently believed that PNe may form through two mechanisms: envelope ejection from single red giants, or common-envelope ejection from close binaries. The relative importance of these mechanisms, particularly as a function of progenitor mass, is not well known.

However, observational evidence is mounting that binary-star processes are a key element in the origin of halo PNe. As noted above, the Jacoby et al. (1997) survey of 133 GCs for PNe brought the total number known to four. These authors pointed out that this is  $3\sigma$  lower than the  $\sim 16$  PNe expected on the basis of the total luminosity of the Galactic GC system, a PN lifetime of  $\sim 2\text{--}3 \times 10^4$  yr, and the assumption that every star produces a visible PN. In order to explain the small number actually observed, Jacoby et al. (1997) suggested that the last assumption may be incorrect in GCs. In fact, the post-asymptotic-giant-branch (post-AGB) stellar evolutionary timescales of individual stars in GCs may be so long that the ejected nebular material has time to disperse before the central star becomes hot enough to ionize it. (This has been called “lazy” evolution by, e.g., Renzini 1981.)

The notion of lazy post-AGB evolution for GC and halo stars is supported by several lines of evidence. First, recent *Hubble Space Telescope* (*HST*) detections of white dwarfs in nearby GCs (Renzini et al. 1996; Cool, Piotto, & King 1996; Richer et al. 1997) indicate that the remnant masses are very low ( $0.50 \pm 0.02 M_{\odot}$ ; see §7). Post-AGB stars of masses  $\lesssim 0.55 M_{\odot}$  have theoretical evolutionary timescales that are much longer than the dissipation timescale for PNe (Schönberner 1983; Vassiliadis & Wood 1994). In addition, Bond & Fullton (1997, 1999) have used star counts of post-AGB stars in the M31 halo to estimate a lifetime of  $\sim 25,000$  years for the portion of the post-AGB evolution from effective temperatures of 5,000 to 10,000 K. Since this is already comparable to the nebular dispersion time, it is unlikely that these halo stars will ionize visible PNe.

The problem then shifts from “Why are there so few PNe in globular clusters?” to “Why are there *any* PNe at all?”. One possibility is that there might be enough scatter in the initial-

mass/final-mass relation to produce occasional remnants that are massive enough to produce PNe. Jacoby et al. (1997), however, proposed that the known GC PNe were formed through close-binary interactions, although they did not propose any specific mechanisms. As mentioned above, the ejection of PNe by close-binary stars is generally attributed to a common-envelope (CE) interaction (Paczýnski 1976; Bond & Livio 1990; see Iben & Livio 1993 for a review). In this scenario, one component of the binary is able to grow to red-giant dimensions, and only then swallows its companion into an envelope surrounding both stars. The orbit spirals down as orbital energy is transferred to the envelope, which can ultimately be spun up and ejected.

Several close-binary evolutionary channels may lead to formation of PNe in GCs, and these PNe may have either single central stars or central stars that are still binaries. In the standard terminology of binary interactions, Case B, Case C, and probably also Case A interactions, are all of interest.

In a Case B interaction, the CE event occurs while the primary is on the first-ascent red giant branch (RGB), and yields a helium white dwarf with a main-sequence secondary. The white-dwarf remnant of a Case B ejection will probably evolve very slowly toward high temperatures, and thus will not form a visible PN (another example of lazy evolution). However, in extreme cases of mass loss during the CE event, a PN with a low-luminosity close-binary central star may be formed (Iben & Tutukov 1993). In a Case C interaction, the CE event does not occur until the primary has reached the AGB, and yields a carbon-oxygen white dwarf with a main-sequence secondary. If the primary’s initial mass was sufficiently high, the CO white dwarf from a Case C ejection will evolve rapidly towards high temperatures, and form a PN with a close-binary central star (Iben & Tutukov 1993). Another possible outcome of either a Case B or C interaction is that the CE event results in a stellar merger. The product of two merged GC stars may be a rapidly rotating red giant (Livio & Soker 1988), which may eventually become a PN by evolving as a higher-mass single star (Yungelson, Tutukov, & Livio 1993). Han, Podsiadlowski, & Eggleton (1995) have used population synthesis simulations to predict the probabilities for these scenarios in a low-mass, low-metallicity field population consisting initially of 50% binaries:  $\sim 10\text{-}15\%$  Case B,  $\sim 1\text{-}4\%$  Case C, and  $\sim 7\%$  mergers (the majority of the binary population having an initial separation too large for any CE interaction to occur).

There is yet another way for binary-star interactions to give rise to halo PNe, especially in a GC. That would be through a Case A interaction, which occurs while both components are on or near the main sequence (and thus a CE event does not occur). Such an interaction could involve a binary that goes into contact (i.e., a W Ursae Majoris system) and coalesces (e.g., Webbink 1976). The coalesced star would appear first as a blue straggler lying near the main sequence but above the cluster’s turnoff, and it would evolve subsequently as a single star of higher mass and shorter evolutionary timescale than stars at the main-sequence turnoff. When such a star ejects its envelope and leaves the AGB, it would produce a relatively massive post-AGB remnant which could form a PN. Many blue stragglers, both in GCs (e.g., Kaluzny et al. 1997 and references therein) and in the field (e.g., Bond & MacConnell 1971) are known binaries, which have so far

avoided merging. This may suggest that mass transfer without a merger is what augments the mass of the blue straggler. It is also possible that binary blue stragglers are the products of a triple-star interaction (Iben & Tutukov 1999) or a binary/binary interaction, with ejection of one star from the system, or with one pair merging and the third star left as a wider companion. In any case, it is now well-known that most GCs contain blue stragglers, presumably formed through collisionally induced mergers that occur in the cluster core, so the above scenario for producing PNe in GCs is plausible (cf. Livio 1993; Stryker 1993; Sills & Bailyn 1999; and references therein). However, given the total numbers of blue stragglers found in GCs, it is not clear that they are sufficient to produce the observed number of GC PNe.

In summary, we have outlined a variety of close-binary evolutionary channels which could produce PNe in halo populations. In some of these scenarios, the central star of K 648 would still be a close binary; in others the star would be a merged remnant. In the field,  $\sim 10\text{--}15\%$  of PNe have photometrically detectable close-binary central stars (Bond & Livio 1990; Bond 2000). In most of these cases, the photometric variability is due to heating of a main-sequence companion (actual eclipses thus not being necessary for detection of binarity). Moreover, the short periods of the binary central stars detected in this manner require the progenitor systems to have evolved through a CE phase. Thus, if we could show that the nucleus of K 648 is such a close binary, this PN would become an important example of CE evolution in the halo population. On this basis, we undertook a photometric monitoring campaign on K 648 with the Wide Field Planetary Camera 2 (WFPC2) camera onboard the *HST* in order to search for a close binary central star.

This paper is organized as follows. In §2, we review relevant observational studies of K 648 and its host cluster, M15. We summarize our new *HST* observations in §3 and in §4 we describe our photometry of the K 648 central star. We derive the fundamental parameters of the central star in §5, and discuss the morphology of the nebula in §6. In §7, we discuss the evolutionary status of the K 648 central star. We conclude in §8.

## 2. Küstner 648 in Messier 15

K 648 lies in a crowded field near the center of M15. In the PN literature, it is also cataloged as Ps 1 and PN G065.0–27.3 (Acker et al. 1992). Radial-velocity measurements confirm its membership in M15 (Joy 1949). In this paper, we will refer to the nebula as K 648, and to its central star explicitly.

O’Dell, Peimbert, & Kinman (1964) presented the first detailed spectrophotometric study of K 648. Subsequent spectrophotometric studies have been reported by Miller (1969), Peimbert (1973), Hawley & Miller (1978), Torres-Peimbert & Peimbert (1979), Barker (1980), and Adams et al. (1984). Johnson, Balick, & Thompson (1979) resolved K 648 with the Very Large Array radio telescope, and found an angular diameter of  $\sim 3''$ . *HST* imaging was carried out at optical wavelengths using the original Wide Field and Planetary Camera (WF/PC1) and the Faint

Object Camera (FOC) by Bianchi et al. (1995). Adams et al. (1984) published an *International Ultraviolet Explorer (IUE)* spectrum, which has been reanalyzed subsequently by others, including Peña, Torres-Peimbert, & Ruiz (1992), Bianchi et al. (1995), and Henry, Kwitter, & Howard (1996). Heber, Dreizler, & Werner (1993) reported on high-resolution ultraviolet spectra of the K 648 central star obtained with *HST* and the Goddard High Resolution Spectrograph (GHRS). McCarthy et al. (1997) analyzed high-resolution, high signal-to-noise optical spectra obtained with HIRES on the Keck 10-m telescope.

The distance and reddening toward K 648 are well constrained owing to its association with M15. The foreground reddening toward M15 is  $E(B - V) = 0.10 \pm 0.01$  mag, as estimated by several independent techniques (Durrell & Harris 1993). The reddening derived from the nebular spectrum of K 648 agrees well with this value. The four published measurements of the Balmer decrement in K 648 tabulated by Adams et al. (1984) yield an average  $H\alpha/H\beta = 3.23 \pm 0.16$ . Adopting the Case B recombination ratios from Osterbrock (1974), and the reddening law of Cardelli, Clayton, & Mathis (1989), we estimate  $E(B - V) = 0.13 \pm 0.05$  mag (assuming an electron temperature of  $1\text{--}2 \times 10^4$  K). Adjusted for the Durrell & Harris (1993) reddening, the *Hipparcos* subdwarf calibration of Reid (1997) yields a true cluster distance modulus  $(m - M)_0 = 15.45 \pm 0.1$  mag, or a distance of  $12.3 \pm 0.6$  kpc.

The chemical abundances of M15 red giants and K 648 have been the subject of numerous studies. Estimates of the metal abundance of red giants in M15 range from  $[\text{Fe}/\text{H}] = -2.4$  (Snedden et al. 1997) up to  $-2.17$  (Zinn & West 1984) and  $-2.12$  (Carretta & Gratton 1997). The abundances of neon and argon in K 648 are subsolar by similar factors of  $\sim 100$  (Barker 1980; Adams et al. 1984). However, K 648 has enhanced oxygen and a very high carbon abundance (Howard et al. 1997), implying that some stellar core material has been ejected into the nebula. It is possible that the K 648 progenitor experienced a “third dredge-up” of core material following a thermal pulse on the AGB (e.g., Buell et al. 1997; Sweigart 1999), even though it has been shown theoretically that third dredge-ups do not occur in model stars with initial masses below  $\sim 1 M_\odot$  (Lattanzio 1989). Hydrodynamical simulations of CE evolution show the development of circulation patterns (Bodenheimer & Taam 1984; Livio & Soker 1988), which could mix core material to the surface (Iben & Livio 1993). Thus close-binary evolution is an alternate mechanism for carbon enrichment in K 648.

### 3. *HST* Observations

Motivated by the above considerations, we searched for periodic light variations of the K 648 central star. As noted, such variations can arise in a close binary from heating effects on a nearby main-sequence companion of the hot central star. Because of the difficulty of accurate photometry of the K 648 central star using ground-based techniques, due to the very crowded field as well as the presence of a bright surrounding PN, we carried out our monitoring with *HST* and its WFPC2 camera.

We observed K 648 during 10 *HST* orbits between 1998 December 15 and 22 UT. We obtained a total of 79 images, with K 648 placed near the center of the PC chip. Most of the observations (57) were optimized for photometric monitoring of the central star, and were made with the broad- and intermediate-band F336W, F439W, F547M, and F814W filters (which we denote  $U$ ,  $B$ ,  $y$ , and  $I$  respectively). The exposure times in these filters were 23, 20, 12, and 14 s, respectively. The  $y$  filter was chosen rather than  $V$  since the former suppresses the strong [O III] 5007 Å nebular emission line, and we included the  $I$  filter since the amplitude of the heating effect on a cool companion of a hot star increases with wavelength. We employed a geometrically increasing series of time spacings that yielded near-optimal sensitivity to periodic light variations over a period range of  $\sim 45$  minutes to  $\sim 7$  days. Some of the exposures (7 of the 57) were, however, affected by intense cosmic-ray hits during spacecraft passages through the South Atlantic Anomaly, and thus were unusable.

The remainder of each of the *HST* orbits was used to obtain observations of K 648 through the F502N, F656N, and F658N narrow-band filters, which are centered on the [O III], H $\alpha$ , and [N II] nebular emission lines. These were obtained in order to study the morphology of the PN at WFPC2 resolution. The multiple exposures obtained in these filters totaled 17.3, 190.3, and 15 minutes, respectively.

#### 4. Central Star Photometry

Aperture photometry of the K 648 central star in each of the usable broad-band images was obtained using DAOPHOT (Stetson 1987). The results showed no significant variability of the nucleus of K 648 over the seven-day *HST* observing campaign, at the  $\lesssim 1\%$  detectability level of our data. Although a positive result would have established the binarity of the central star, our negative result does not rule it out. The nucleus could still be a binary, either viewed close to pole-on, or of sufficiently large orbital period and separation for the heating effects to be negligible. If the star is a binary, a precise lower limit on its possible orbital period is difficult to state based on our null detection, since the limit depends both on the viewing geometry and the radius of the putative companion. However, the lower limit is probably of order several days.

We then combined all of the usable images in each broad- and intermediate-band filter using a median algorithm, and rederived the aperture photometry from the resulting composite images. Due to the strong cluster background in our frames, it was not necessary to apply charge-transfer-efficiency (CTE) corrections. Aperture corrections were determined from several nearby bright, isolated stars in the PC images. The errors associated with the aperture corrections ( $\sim 1\%$ ) dominate over the DAOPHOT-reported Poisson errors ( $\sim 0.1\%$ ) in the magnitudes from the combined images. By a careful comparison of each broad-band image with the H $\alpha$  image, we estimate that the magnitudes are contaminated by nebular line emission at no more than the  $\sim 1\%$  level in  $U$ ,  $B$ , and  $y$ , and  $\sim 3\%$  in  $I$ . The central star colors were then transformed to the standard Johnson-Kron-Cousins  $UBVI$  system, according to the prescription of Holtzman et al. (1995). The

calibrated magnitudes of the K 648 central star are summarized in Table 1. The systematic errors of the calibrated magnitudes and colors are of order 2–3% (Holtzman et al. 1995). The conversion from *UBVI* magnitudes to absolute fluxes, also given in Table 1, was calculated according to Bessell, Castelli, & Plez (1998).

In order to study the spectral energy distribution (SED) of the central star, we will consider both the *HST*/WFPC2 flux data and the ultraviolet spectrum. As discussed by Adams et al. (1984), flux contamination in the large-aperture *IUE* spectrum from neighboring stars and the nebula is small at  $\lambda < 1800 \text{ \AA}$ . Therefore, we restricted our analysis to the short-wavelength spectrum. We used the highest-S/N *IUE* observation available in the archive maintained at STScI, image number SWP 17069. The mean fluxes in 100  $\text{\AA}$ -wide passbands centered at  $\lambda = 1300, 1450, 1650$  and  $1800 \text{ \AA}$  are listed in Table 1. These passbands were selected to avoid obvious emission and absorption lines, and thus represent the central star’s continuum.

The K 648 central star was also observed with the *HST*’s Faint Object Spectrograph (FOS). The unpublished *HST*/FOS spectrum was kindly provided in electronic form by R. Bohlin (2000), calibrated on the white dwarf scale according to Bohlin (1996) and Bohlin, Lindler, & Keyes (1995). The uncertainty in FOS absolute fluxes are estimated to be  $\sim 5\%$  for this spectrum. In a direct comparison at short wavelengths, the *IUE* spectrum appears to suffer from a  $\sim 15\%$  loss of flux relative to the FOS data, possibly due to misalignment in the slit. The mean *IUE* and *HST*/FOS fluxes at  $\lambda = 1300, 1450, 1650$  and  $1800 \text{ \AA}$  are compared in Table 1. Given the flux discrepancy and the superior resolution of *HST*/FOS, we employ only the FOS data in our analysis of the SED below. The average continuum flux data points are sufficient to constrain the various physical parameters that we seek from the central star’s SED.

We adopt the reddening law of Cardelli, Clayton, & Mathis (1989) to deredden the *HST*/WFPC2 and FOS flux data. The ratios of total extinction ( $A_\lambda$ ) to the total visual extinction ( $A_V$ ) for each of our flux data points are listed in Table 1. As noted above, the reddening for M15 is known to be  $E(B - V) = 0.10 \pm 0.01$  mag from Durrell & Harris (1993). Having assumed  $R_V = A_V/E(B - V) = 3.1$ , we previously estimated the cluster’s distance using a visual extinction of  $A_V = 0.31$  mag. In our analysis below, we will consider possible variations in the extinction law ( $R_V$ ). Thus, for simplicity, we will hold  $A_V = 0.31$  mag constant so that the cluster is always assumed to be at the same distance. Plausible variations in  $R_V$  while  $A_V$  is held constant lead to only small changes in  $E(B - V)$ , but relatively large changes in the dereddened far-ultraviolet fluxes. In our analysis below, we will assume that the K 648 central star has the same reddening as the cluster, but consider also the possibility that the central star is additionally reddened (i.e., perhaps by its own ejected material).

## 5. Luminosity, Effective Temperature, and Mass of the K 648 Central Star

With our new *HST*/WFPC2 and FOS data and the recent *Hipparcos*-calibrated distance to M15, it is worth revisiting the luminosity and color-temperature calculation for the K 648 central star given by Adams et al. (1984). Previous ground-based photometry of the nucleus required large and uncertain corrections for nebular contamination, which are of course unnecessary with the WFPC2 data. Figure 1 shows the SED of the central star. We plot both the new *UBVI* points from our WFPC2 observations and the four points from the short-wavelength FOS data.

Our approach is to fit Lejeune et al. (1997) model stellar spectra<sup>2</sup> to the flux data summarized in Table 1. Each model spectrum is tabulated as wavelength ( $\lambda$ ) in nm and flux moment ( $H_\nu$ ) in  $\text{erg s}^{-1} \text{cm}^{-2} \text{Hz}^{-1}$ , which we convert to flux using the formula

$$f_\lambda = \frac{0.4cH_\nu}{\lambda^2}, \quad (1)$$

where  $c$  is the speed of light in  $\text{nm s}^{-1}$ , and the units of  $f_\lambda$  are  $\text{erg s}^{-1} \text{cm}^{-2} \text{\AA}^{-1}$ . At Earth the flux from the star is given by

$$F_\lambda = \left( \frac{\pi R^2}{D^2} \right) f_\lambda, \quad (2)$$

where  $R$  is the radius of the star and  $D$  is its distance. In our case,  $D$  is known,  $F_\lambda$  has been measured (Table 1), and  $f_\lambda$  can be obtained as a function of  $T_{\text{eff}}$  from the Lejeune et al. model spectra as given above. Thus, with multi-wavelength data, we can solve simultaneously for the stellar radius and effective temperature. We adopt the model fluxes at the effective wavelengths of the various bandpasses. The luminosity of the central star ( $L$  in units of  $\text{erg s}^{-1}$ ) is then given by

$$L = 4\pi R^2 \sigma T_{\text{eff}}^4 = 4\pi^2 R^2 \int_0^\infty f_\lambda d\lambda. \quad (3)$$

In our first round of fitting, a  $\chi^2$  minimization is used to find  $R$ ,  $T_{\text{eff}}$ , and the extinction ratio  $R_V$ . We employ model spectra with  $[\text{Fe}/\text{H}] = -2.0$ , which corresponds roughly to the metallicity of M15 red giants. The very low metallicity assumed here may not be appropriate for the central star if its photosphere contains material dredged up from the core, so we also fit using model spectra with  $[\text{Fe}/\text{H}] = 0.0$ , which however yielded the same results. We conclude that the color temperature is insensitive to different assumptions for the K 648 central star photospheric abundances. In this round of fitting, the  $1\sigma$  confidence intervals are  $T_{\text{eff}} = 37,500$  to  $50,000$  K, and  $\log(L/L_\odot) = 3.71$  to  $4.11$ . However, the upper limits are set by the highest temperature model spectrum fitted and not the  $\chi^2$  statistic. The best-fit for  $R_V$  is quite low,  $R_V = 2.0_{-0.2}^{+0.4}$  ( $1\sigma$  errors), but within the range of known values ( $R_V = 2$  to  $5$ ; Fitzpatrick 1999).

---

<sup>2</sup>We use their “corrected” model spectra and adopt  $\log g = 5.0$ , for which model spectra are provided for the entire range of effective temperatures of interest. The specific choice of  $\log g$  has a negligible effect on our derived results. In order to convert to astronomical units, we assume values for the Sun of  $\log L_\odot = 33.582$  and  $\log R_\odot = 10.842$ , where  $L_\odot$  and  $R_\odot$  are in units of  $\text{erg s}^{-1}$  and cm, respectively.

We considered the possibility that the K 648 central star is reddened in excess of the mean cluster reddening, perhaps due to dust in the surrounding nebula. This possibility is raised by our measured  $B - V$  color of  $-0.13$ . For example, the Lejeune et al. intrinsic color of  $-0.31$  at 40,000 K then suggests  $E(B - V) \simeq 0.18$  mag. We also recall that the nebular Balmer decrement, as discussed in §2, indicates  $E(B - V) = 0.13 \pm 0.05$  mag. However, the central star’s  $U - B$  and  $V - I$  colors and the nebular value are all consistent within their errors with the adopted  $E(B - V) = 0.10$  mag. In any case, we note that the effect of increasing the K 648 central star reddening will be to *increase* the derived stellar luminosity and mass, which will only strengthen our conclusions about its evolutionary history (see §7).

In a second round of fitting, a  $\chi^2$  minimization is used to find  $R$ ,  $T_{\text{eff}}$ , and the reddening  $E(B - V)$ , which is allowed to be larger than the cluster’s foreground reddening of  $E(B - V) = 0.10$ . In this case, we assume the “standard” extinction ratio of  $R_V = 3.1$ . A  $\chi^2$  minimization yields the  $1\sigma$  confidence intervals of  $T_{\text{eff}} = 33,000$  to 47,500 K and  $\log(L/L_\odot) = 3.61$  to 4.02 dex. The best-fit reddening is  $E(B - V) = 0.13^{+0.02}_{-0.01}$  ( $1\sigma$  errors). This is in excellent agreement with that found using the nebular Balmer decrement, as noted above.

Not surprisingly, our analysis of the SED only weakly constrains the effective temperature of the central star (because even the far-UV points are essentially on the Rayleigh-Jeans tail). The stellar effective temperature is almost entirely unconstrained by our new optical flux data, except that the lack of a perceptible Balmer jump weakly favors a high temperature. The far-UV data are sensitive to the adopted reddening and reddening law, in addition to the effective temperature of the central star.

Fortunately, spectroscopic analyses based on absorption-line measurements can provide much tighter constraints. Analyses of this type have yielded  $T_{\text{eff}} = 37,000$  K (Heber et al. 1993) and  $T_{\text{eff}} = 43,000 \pm 2,000$  K (McCarthy et al. 1997; Méndez 1999), based on UV and optical spectra, respectively. These spectral-line temperatures are consistent with our color temperature, but more accurate, and we give them high weight. They are also consistent with the value of  $38,000 \pm 4,000$  K adopted by Adams et al. (1984) on the basis of the Zanstra and Stoy nebular methods and their analysis of the optical/UV energy distribution. We therefore adopt an effective temperature of  $T_{\text{eff}} = 40,000 \pm 3,000$  K.

With the temperature fixed to  $T_{\text{eff}} = 40,000$  K, and allowing  $R_V$  to vary, we find a best-fit of  $R_V = 2.3$ . For  $R_V = 3.1$  and allowing  $E(B - V)$  to vary while the temperature is held fixed, we find a best-fit of  $E(B - V) = 0.13$ . Given the low value of  $R_V = 2.3$  found, the scenario in which the K 648 central star is reddened slightly more than the mean reddening of the cluster is probably preferred. However, both scenarios yield consistent results for the luminosity and radius of the K 648 central star. Our adopted effective temperature of  $T_{\text{eff}} = 40,000 \pm 3,000$  K corresponds  $\log(L/L_\odot) = 3.78 \pm 0.08$ , and  $R/R_\odot = 1.61^{+0.11}_{-0.06}$ . Figure 1 shows the SED for a standard reddening law of  $R_V = 3.1$  and a reddening of  $E(B - V) = 0.13$ .

An estimate of the K 648 central star mass follows from theoretical calculations of post-AGB

evolutionary tracks (Paczýnski 1971; Schönberner 1979, 1983; Vassiliadis & Wood 1994). The well-known luminosity/core-mass relation is one of the basic predictions in AGB and post-AGB stellar evolution theory. Vassiliadis and Wood find a luminosity/core-mass relation of  $L/L_{\odot} = 56694(M_c/M_{\odot} - 0.5)$ , independent of metallicity, and applicable to both hydrogen- and helium-burning tracks. This relation predicts the luminosities of their individual post-AGB tracks with an rms scatter of  $\pm 0.02$  dex in  $\log(L/L_{\odot})$ . Using this formula, we find that the mass of the K 648 central star is  $M = 0.60 \pm 0.02 M_{\odot}$ , where the uncertainty does not include the systematic error associated with the theoretical luminosity/core-mass calibration (which is comparable to the statistical error).

For our derived mass and radius, the surface gravity of the central star is predicted to be  $\log g = 3.8$ . This agrees well with both Heber et al. (1993) and McCarthy et al. (1997), who found  $\log g$ 's of 4.0 and 3.9, respectively, from their spectroscopic analyses.

## 6. Morphology of the Nebula

K 648 is barely resolved optically from the ground (see, for example, Górný et al. 1999). *HST* imaging with the pre-repair WF/PC1 was reported by Bianchi et al. (1995). Our new WFPC2 data confirm the basic morphological features discussed by Bianchi et al., but also provide new information revealed by the even higher spatial resolution of the repaired *HST*.

K 648 shows three main structural features, which are revealed clearly in our new images and can be described approximately as follows: (1) a very bright, hollow, inner elliptical shell, with outer major and minor axes of  $0''.8$  and  $0''.6$ ; (2) a larger, somewhat fainter, and fairly sharp-edged elliptical shell of dimensions  $3''.1 \times 2''.7$ ; and (3) a much fainter, diffuse elliptical halo that fades away gradually with radius but can be detected out to dimensions of at least  $6''.5 \times 5''.5$ . The corresponding dimensions in parsecs are: inner shell  $0.05 \times 0.04$  pc, outer shell  $0.19 \times 0.16$  pc, and faint halo  $0.38 \times 0.33$  pc. These three features are illustrated in our deep WFPC2  $H\alpha$  image of K 648 displayed in Figure 2, where the image stretch is logarithmic and has been adjusted to show the faint outer halo and (overexposed in this stretch) the outer sharp-edged elliptical shell. The structure of the bright inner shell is represented in Figure 2 by superposed isophotes. The two bright inner elliptical shells seen in K 648 are a typical morphological feature of many “elliptical” PNe (e.g., Balick 1987). Large faint halos are also often seen when sufficiently deep images are available.

The most remarkable feature of the morphology, seen most clearly for the first time in our WFPC2 images, is a bright arc on the northwestern end of the nebula’s major axis, located just inside the edge of the outer bright elliptical shell. This arc is especially prominent in the light of [N II], and is seen as well in  $H\alpha$  and [O III]. A corresponding feature at the other end of the major axis does not appear to be present, although two fairly bright stars are unfortunately superposed at exactly that position. Figure 3 is a false-color image that illustrates this feature.

At first sight, one might interpret the arc as a bow shock, arising from the high velocity of M15 through the interstellar medium (ISM). The PN in the globular cluster M22 shows strong evidence for an interaction with the ISM in ground-based images (Borkowski, Tsvetanov, & Harrington 1993), and an ISM interaction is also suspected involving the PN in NGC 6441 based on *HST* WFPC2 images (Jacoby et al. 1997). However, we believe that an interaction is an unlikely explanation for the arc in K 648, because the faint outer halo of the PN appears completely undisturbed. Knowledge of the absolute proper motion of M15 would also be useful in assessing this possibility, but recent ground-based studies have not even agreed on the signs of the right-ascension and declination components (Scholz et al. 1996 and references therein). However, three out of the four recent studies summarized by Scholz et al. have found a southward declination component. In this case, the arc-like feature is on the wrong side of K 648 for it to be a bow shock. Actually it would be surprising to find evidence for an ISM interaction in K 648, since M15 lies  $\sim 5600$  pc below the Galactic plane, compared with 400 pc for M22 and 1000 pc for NGC 6441.

The arc feature is probably composed of “FLIERS” (fast low-ionization emission regions), which are a phenomenon seen in many double-shell elliptical PNe. FLIERS often occur at or just inside the outer elliptical shell, and often near the ends of the major axis, just as seen in K 648. The origin of FLIERS is still uncertain (see Balick et al. 1998 and references therein). It is somewhat unusual to find FLIERS at only one end of the major axis, as in K 648. However, M 2-2 is one example of a field PN that exhibits a concentration of FLIERS on only one side of the nebula (Manchado et al. 1996, pp. 107 and 147). M 2-2 even shows a faint “neck” connecting its inner and outer elliptical shells, along the major axis in the direction of the FLIERS, which is seen also in our Figure 3.

In summary, the morphology of K 648 is fairly typical of that seen in many elliptical PNe, with the only somewhat unusual feature being a concentration of FLIERS at one end of its major axis. There is no strong evidence for interaction with the interstellar (or intracluster) medium. Whether the morphologies of all elliptical PNe are due to binary-star interactions has been debated vigorously (e.g., Kastner, Soker, & Rappaport, eds., 2000), but the answer remains uncertain. However, nebular ejection as a consequence of a CE interaction, or the enhanced rotation of the AGB progenitor that would result from tidal spinup in a binary system or from a stellar merger, are natural ways to produce the density contrast seen in elliptical PNe. Thus the morphology of K 648 may suggest that it is descended from a close-binary progenitor.

## 7. The Anomalous Mass of the K 648 Central Star

The mass we have derived for the K 648 central star,  $M = 0.60 \pm 0.02 M_{\odot}$ , is anomalously high for a stellar remnant in an old globular cluster (or in the Galactic halo), as shown by several recent *HST*/WFPC2 studies. Richer et al. (1997) observed a large number of white dwarfs in the GC M4. These authors found the M4 distance modulus by fitting subdwarfs to the cluster main

sequence, and then derived a model-dependent mean white dwarf mass of  $M_{\text{WD}} = 0.51 \pm 0.03 M_{\odot}$ . Cool et al. (1996) observed a smaller number of white dwarfs in NGC 6397. They also derived the cluster distance modulus by main-sequence fitting, and estimated a model-dependent white dwarf mass of  $M_{\text{WD}} = 0.55 \pm 0.05 M_{\odot}$ . Renzini et al. (1996) observed the white dwarf sequence in the globular cluster NGC 6572. However, instead of measuring the white dwarf masses based on the cluster distance, these authors adopted 5 field halo white dwarfs with measured trigonometric parallaxes as calibrators. The halo white dwarfs have a mean  $M_{\text{WD}} = 0.51 \pm 0.01 M_{\odot}$ , based on fitting to theoretical cooling curves. From this calibration, Renzini et al. derived a distance modulus of  $(m - M)_0 = 13.05 \pm 0.10$  mag by fitting to the cluster white-dwarf sequence. The Renzini et al. (1996) distance modulus compares with  $(m - M)_0 = 13.23 \pm 0.10$  mag found by Reid (1997) who fit subdwarfs to the main sequence (both authors adopted the same reddening). We can recalculate the masses of white dwarfs in NGC 6572 relative to the main sequence as follows. Referring to the same model white dwarf sequences (see Bergeron, Ruiz, & Leggett 1997) employed by Cool et al. (1996) and Richer et al. (1997), we find that at a fixed color, the white dwarf mass scales with absolute magnitude according to  $M_V \propto 2.75 M_{\text{WD}}$ . Allowing for the Reid (1997) distance, the absolute magnitude of the cluster white dwarfs shift by  $\Delta M_V = -0.18$  mag, which yields a shift of  $\Delta M_{\text{WD}} = -0.06 M_{\odot}$  relative to the local calibrators employed by Renzini et al. (1996). Thus, we find  $M_{\text{WD}} = 0.46 \pm 0.04 M_{\odot}$  for the mass of white dwarfs in NGC 6572, where the associated error is dominated by the uncertainty in the distance modulus.

Taking the weighted average of these three measurements in GCs, we derive a best estimate for a mean globular cluster white-dwarf mass of  $M_{\text{WD}} = 0.50 \pm 0.02 M_{\odot}$ . This mass is consistent with the mean mass of the halo field white dwarfs selected by Renzini et al. (1996) as calibrators. Thus we conclude that the masses of white dwarfs in GCs and in the halo are significantly lower than the mass we estimate for the K 648 central star.

Yet another argument for a high mass for the K 648 nucleus arises from a comparison of nebular and stellar evolutionary timescales (see, e.g., Bianchi et al. 1995; Buell et al. 1997). If we assume a nebular angular radius of  $r \simeq 1''.5$  (see §6; this radius refers to the nebula’s outer bright elliptical shell, which we interpret as having arisen at the main ejection event whose onset occurred at the end of the AGB phase), and adopt a typical PN expansion rate of  $v_{\text{exp}} \simeq 20 \text{ km s}^{-1}$ , then the dynamical age of K 648 is

$$\tau_{\text{dyn}} \simeq 4400 \text{ yr} \left( \frac{r}{1''.5} \right) \left( \frac{v_{\text{exp}}}{20 \text{ km s}^{-1}} \right)^{-1}. \quad (4)$$

To our knowledge, post-AGB evolutionary models do not exist for the low metallicities and low progenitor masses relevant for K 648. However, indications are that the nucleus can evolve from the AGB to a temperature of  $\sim 40,000$  K within  $\sim 4400$  yr only if its mass exceeds  $\approx 0.59 M_{\odot}$  (see, e.g., Schönberner 1983; Vassiliadis & Wood 1994; Blöcker & Schönberner 1997; and references therein). A slightly lower mass near  $0.56 M_{\odot}$  is possible for a helium-burning central star, according to the Vassiliadis & Wood calculations. However, at the considerably lower core masses implied by the *HST* observations of white dwarfs in GCs, the evolutionary timescales are likely to be extremely

leisurely and greatly exceed  $\tau_{\text{dyn}}$ .

The weight of the evidence thus suggests strongly that the mass of the K 648 central star is unusually high compared to the normal remnants of halo and GC stars. Interestingly, the central star of the PN in M22 also appears to be much more luminous than would be expected if it is the remnant of a turnoff star of  $\sim 0.8 M_{\odot}$ , according to an analysis of ground-based and *IUE* spectra by Harrington & Paltoglou (1993). However, their determination of the star’s high  $L/L_{\odot}$  depends on the uncertain  $T_{\text{eff}}$  of the star. Moreover, this object presents additional evolutionary puzzles because of the extremely hydrogen-deficient composition of its nebula but not of the central star itself, the latter being a helium-rich sdO star.<sup>3</sup>

### 7.1. Mass Augmentation in a Close Binary?

We believe the most likely explanation for the unusually high mass of the K 648 nucleus is that the star has experienced mass augmentation at some point in its evolutionary history, which would be explained most naturally through an interaction in a close binary system.

In M15 the current main-sequence turnoff mass is  $\sim 0.80 M_{\odot}$  (Reid 1997). The initial mass of the K 648 progenitor that would be implied by a current mass of  $0.60 M_{\odot}$  is quite uncertain, because the theoretical initial-final mass relation depends on metallicity, and we require an extrapolation to lower metallicities than provided by the available post-AGB models. However, by inspection of the lowest-metallicity post-AGB tracks of Vassiliadis & Wood (1994), we conclude that the most probable initial mass of the K 648 progenitor is  $M_i \lesssim 1.0 M_{\odot}$ . In this case, the original  $0.80 M_{\odot}$  star needs to have experienced a modest  $\sim 25\%$  mass augmentation, and then evolved as a higher-mass star to become K 648. This higher mass may also be consistent with the high carbon abundances in K 648, which, as noted above, may have resulted from the dredge-up of core material due to the thermal-pulse instability on the AGB (Lattanzio 1989) of a star of  $\sim 1 M_{\odot}$ .

If the PNe in GCs arise from close binaries that merged on the main sequence, then they are the descendants of blue stragglers. This may lead to a problem in the predicted numbers of PNe in GCs, as shown by the following rough estimate. If we assume that the total number of blue stragglers in GCs is of order 100 per cluster, or about  $10^4$  in total, that each has a lifetime of  $\sim 10^9$  yr, and that each PN lives  $\sim 2.5 \times 10^4$  yr, we predict there should be only  $\sim 0.25$  PNe in the GC system. This suggests that the blue stragglers (i.e., the Case A mergers) may not be able to account for all four PNe known in GCs. Scenarios in which the PN is ejected during a Case B

---

<sup>3</sup>For completeness, we note that the luminosities of the central stars of the PNe in Pal 6 and NGC 6441 suggest that they may not be as massive as the nuclei of K 648 or the PN in M22. However, the luminosities of these central stars are not known with great accuracy, so the constraints on their masses are not tight (see discussion in Jacoby et al. 1997). Improved observations of these two objects, along with stronger evidence that the PN associated with Pal 6 is actually a cluster member, would be very useful.

or C CE interaction, leaving a nucleus that is still a binary (e.g., Han et al. 1995), suffer from a failure to predict the observed high luminosity of the K 648 nucleus. This channel could, however, account for about two fainter PN nuclei in the GC system, perhaps not unlike those in NGC 6441 and Pal 6. Han et al. also predict that  $\sim 7\%$  of the stars in an old population will merge in CEs, leaving red giants of higher masses; these merger products could then evolve later to produce PN nuclei as massive as K 648. This formation channel could produce about one PN in the entire GC system. It thus appears that close-binary evolution may be able to account for the observed small number of PNe in GCs, and that merger scenarios are most likely to produce a high-mass central star like that of K 648.

## 7.2. Stochastic Scatter in the Initial-Mass Final-Mass Relation?

The mass of the K 648 central star is anomalously high compared to the mean remnant mass in GCs. In the previous subsection we explored scenarios involving binary interactions. Binary evolution allows us to retain the assumption of a unique, single-valued relationship between initial and final stellar masses for the evolution of single stars. In this subsection we explore whether the high mass of K 648 instead simply indicates a large scatter in the initial-final mass relationship.

If the discrepancy between the mass of the K 648 nucleus and the mean mass of white dwarfs in GCs were due to stochastic mass loss, then the standard deviation in the final masses would be of order  $0.1 M_{\odot}$ . The best-observed white-dwarf sequence in a GC is that of Richer et al. (1997), whose data do not exclude a scatter this large given the photometric errors.

Reid (1996) has estimated the initial and final masses of white dwarfs in several open clusters, and argued for appreciable stochastic scatter in the relationship. For the Hyades and Praesepe clusters with initial masses of  $M_i \sim 2.5 M_{\odot}$ , he finds a mean final mass of  $M_f = 0.69 M_{\odot}$ , with a standard deviation of  $0.13 M_{\odot}$ .

Thus we cannot rule out the possibility that the anomalously high mass of the K 648 nucleus is due to stochastic mass loss. However, as discussed above, binary-star processes appear to be a sufficient explanation. In fact, the scatter in final masses reported at higher progenitor masses could in itself also arise from close-binary interactions, as we have suggested for the case of K 648.

## 8. Conclusion

K 648 in the GC M15 is the prototype of PNe formed by low-mass and low-metallicity progenitors. We have presented new observations of K 648 obtained with *HST* and the WFPC2 camera, from which (combined with our analysis and discussion of previously published information) we have calculated the central star’s temperature, luminosity, and mass. We have also presented the morphology of K 648 with unprecedented resolution. It is a fairly typical

double-shelled elliptical PN, surrounded by a fainter smooth outer halo. Its only unusual structural feature is a bright arc at one end of the major axis, which is bright in [N II] and is probably a collection of FLIERs such as seen in other elliptical PNe.

The derived mass of  $0.60 M_{\odot}$  is consistent with that required for the remnant to be able to evolve to high enough temperature to ionize its surrounding envelope before the envelope has had time to dissipate. However, this mass is significantly higher than those of white dwarfs in GCs. We outlined several possible evolutionary scenarios through which mass transfer or mergers may lead to a luminous PN central star in a GC.

In some of these scenarios, the central star would still be a close binary. However, our WFPC2 observations revealed no significant photometric variability over periods of 45 minutes to 7 days. This null result does not rule out the possibility that the nucleus is a binary, either seen close to pole-on, or having an orbital period of more than several days. However, we suggest that the present central star is probably descended from a binary that merged on the main sequence or in a common-envelope interaction.

Support for this work was provided by NASA through grant number GO-06751.01-95A from the Space Telescope Science Institute, which is operated by the Association of Universities for Research in Astronomy, Inc., under NASA contract NAS5-26555. Brian Warner provided support for this program at a critical time. Laura Fullton and Karen Schaefer assisted in the initial discussion and planning of the observations, and Denise Taylor dealt cheerfully with implementation of the complex and demanding *HST* scheduling requirements. Roberto Méndez and Ulrich Heber sent useful private communications. We thank Ralph Bohlin for providing his unpublished, calibrated *HST*/FOS spectrum of the K 648 central star.

## REFERENCES

- Acker, A., Ochsenbein, F., Stenholm, B., Tylenda, R., Marcout, J., & Schohn, C. 1992, Strasbourg-ESO Catalog of Galactic Planetary Nebulae (Garching: ESO)
- Adams, S., Seaton, M.J., Howarth, I.D., Auriere, M., & Walsh, J.R. 1984, MNRAS, 207, 471
- Balick, B. 1987, AJ, 94, 671
- Balick, B., Alexander, J., Hajian, A. R., Terzian, Y., Perinotto, M., & Patriarchi, P. 1998, AJ, 116, 360
- Barker, T. 1980, ApJ, 237, 482
- Bergeron, P., Ruiz, M.T., & Leggett, S.K. 1997, ApJS, 108, 339
- Bessell, M., Castelli, F., & Plez, B. 1998, A&A, 333, 231
- Bianchi, L., Ford, H., Bohlin, R., Paresce, F., & De Marchi, G. 1995, A&A, 301, 537
- Blöcker, T., & Schönberner, D. 1997, A&A, 324, 991
- Bodenheimer, P., & Taam, R.E. 1984, ApJ, 280, 771
- Bohlin, R. C., Lindler, D. J., & Keyes, C. D. 1995, FOS Instrument Science Report CAL/FOS-144
- Bohlin, R. C. 1996, AJ, 111, 1743
- Bohlin, R. C. 2000, private communication
- Bond, H.E. 2000, in Asymmetrical Planetary Nebulae II: From Origins to Microstructures, ed. J. Kastner, N. Soker, & S. Rappaport, 115
- Bond, H.E., & Fullton, L.K. 1997, BAAS, 29, 843
- Bond, H.E., & Fullton, L.K. 1999, in Eleventh European Workshop on White Dwarfs, ed. J.-E. Solheim & E. G. Meistas (San Francisco: Astronomical Society of the Pacific), 439
- Bond, H.E., & Livio, M. 1990, ApJ, 355, 568
- Bond, H.E., & MacConnell, D.J. 1971, ApJ, 165, 51
- Borkowski, K. J., Tsvetanov, Z., & Harrington, J. P. 1993, ApJ, 402, L57
- Buell, J.F., Henry, R.B.C., Baron, E., & Kwitter, K.B. 1997, ApJ, 483, 837
- Cardelli, J.A., Clayton, G.C., & Mathis, J.S. 1989, ApJ, 345, 245
- Carretta, E., & Gratton, R.G. 1997, A&AS, 121, 95
- Cool, A.M., Piotto, G., & King, I.R. 1996, ApJ, 468
- Durrell, P.R., & Harris, W.E. 1993, AJ, 105, 1420
- Fitzpatrick, E. L., 1999, PASP, 111, 63
- Gillett, F.C., Jacoby, G.H., Joyce, R.R., Cohen, J.G., Neugebauer, G., Soifer, B.T., Nakajima, T., & Matthews, K. 1989, ApJ, 338, 862

- Górny, S. K., Schwarz, H. E., Corradi, R.L.M., & Van Winckel, H. 1999, *A&AS*, 136, 145
- Han, Z., Podsiadlowski, P., & Eggleton, P.P. 1995, *MNRAS*, 272, 800
- Harrington, J. P., & Paltoglou, G. 1993, *ApJ*, 411, L103
- Hawley, S., & Miller, J. 1978, *ApJ*, 220, 609
- Heber, U., Dreizler, S., & Werner, K. 1993, *Acta Astronomica*, 43, 337
- Henry, R.B.C., Kwitter, K.B., & Howard, J.W. 1996, *ApJ*, 458, 215
- Holtzman, J. et al. 1995, *PASP*, 107, 156
- Howard, J.W., Henry, R.B.C., & McCartney, S. 1997, *MNRAS*, 284, 465
- Iben, I., & Livio, M. 1993, *PASP*, 105, 1373
- Iben, I., & Tutukov, A. 1993, *ApJ*, 418, 343
- Iben, I., & Tutukov, A. 1999, *ApJ*, 511, 324
- Jacoby, G.H., Morse, J.A., Fullton, L.K., Kwitter, K.B., & Henry, R.B.C. 1997, *AJ*, 114, 2611
- Johnson, H. M., Balick, B., & Thompson, A.R. 1979, *ApJ*, 233, 919
- Joy, A. H. 1949, *ApJ*, 110, 105
- Kaluzny, J., Kubiak, M., Szymanski, M., Udalski, A., Krzeminski, W., Mateo, M., & Stanek, K. 1997, *A&AS*, 122, 471
- Kastner, J. H., Soker, N., & Rappaport, S. A., eds. 2000, *Asymmetrical Planetary Nebulae II: From Origins to Microstructures* (San Francisco: Astronomical Society of the Pacific)
- Küstner, W. 1921, *Veröff. Univ. Sternwarte Bonn*, 15
- Lattanzio, J. 1989, *ApJ*, 344, L25
- Lejeune, T., Cuisinier, F., & Buser, R. 1997, *A&AS*, 125, 229
- Livio, M. 1993, in *Blue Stragglers*, ed. R. A. Saffer (San Francisco: Astronomical Society of the Pacific), 3
- Livio, M., & Soker, N. 1988, *ApJ*, 329, 764
- Manchado, A., Guerrero, M.A., Stanghellini, L., & Serra-Ricart, M. 1996, *The IAC Morphological Catalog of Northern Galactic Planetary Nebulae*, (Tenerife: IAC)
- McCarthy, J. K., Méndez, R.H., Becker, S., Butler, K., & Kudritzki, R.-P. 1997, in *IAU Symp. 180, Planetary Nebulae*, ed. H. Habing & H. Lamers (Dordrecht: Kluwer), 122
- Méndez, R. H. 1999, private communication
- Miller, J.S. 1969, *ApJ*, 157, 1215
- O'Dell, C., Peimbert, M., & Kinman, T. 1964, *PASP*, 100, 620
- Osterbrock, D.E. 1974, *Astrophysics of Gaseous Nebula and Active Galactic Nuclei* (University Science Books, Mill Valley), 66

- Paczýnski, B. 1971, *Acta Astron.*, 21, 417
- Paczýnski, B. 1976, in *IAU Symp. 73, Structure and Evolution of Close-Binary Systems*, ed. P. Eggleton, S. Mitton, & J. Whelan (Dordrecht: Reidel), 75
- Pease, F. G. 1928, *PASP*, 40, 342
- Peimbert, M. 1973, *Mem. Soc. Roy. Sci. Leige*, 6<sup>e</sup> Ser., 5, 307
- Peimbert, M. 1978, *IAU Symp. 78, Planetary Nebulae*, ed. Y. Terzian (Dordrecht: Reidel), 215
- Peña, M., Torres-Peimbert, S., & Ruiz, M.T. 1992, *A&A*, 265, 757
- Reid, I.N. 1996, *AJ*, 111, 2000
- Reid, I.N. 1997, *AJ*, 114, 161
- Renzini, A. 1981, *Physical Processes in Red Giants*, ed. I. Iben & A. Renzini (Dordrecht: Reidel), 431
- Renzini, A. et al. 1996, *ApJ*, 465, L23
- Richer, H. B., et al. 1997, *ApJ*, 484, 741
- Scholz, R.-D., Odenkirchen, M., Hirte, S., Irwin, M. J., Börngen, F., & Ziener, F. 1996, *MNRAS*, 278, 251
- Schönberner, D. 1979, *A&A*, 79, 108
- Schönberner, D. 1983, *ApJ*, 272, 708
- Sills, A., & Baily, C. D. 1999, *ApJ*, 513, 428
- Snedden, C., Kraft, R.P., Shetrone, M.D., Smith, G.H., Langer, G.E., & Prosser, C.F. 1997, *AJ*, 114, 1964
- Stetson, P. 1987, *PASP*, 99, 191
- Stryker, L. L. 1993, *PASP*, 105, 1081
- Sweigart, A.V. 1999, *IAU Symp. 190, New Views of the Magellanic Clouds*, ed. Y-H. Chu, N. B. Suntzeff, J. Hesser, & D. Bohlender (astro-ph/9909470)
- Torres-Peimbert, S. & Peimbert, M. 1978, *Rev. Mex. Ast. Astrofis.*, 4, 341
- Vassiliadis, E., & Wood, P. 1994, *ApJS*, 92, 125
- Webbink, R. F. 1976, *ApJ*, 209, 829
- Yungelson, L.R., Tutukov, A.V., & Livio, M. 1993, *ApJ*, 418, 794
- Zinn, R., & West, M.J. 1984, *ApJS*, 55, 45

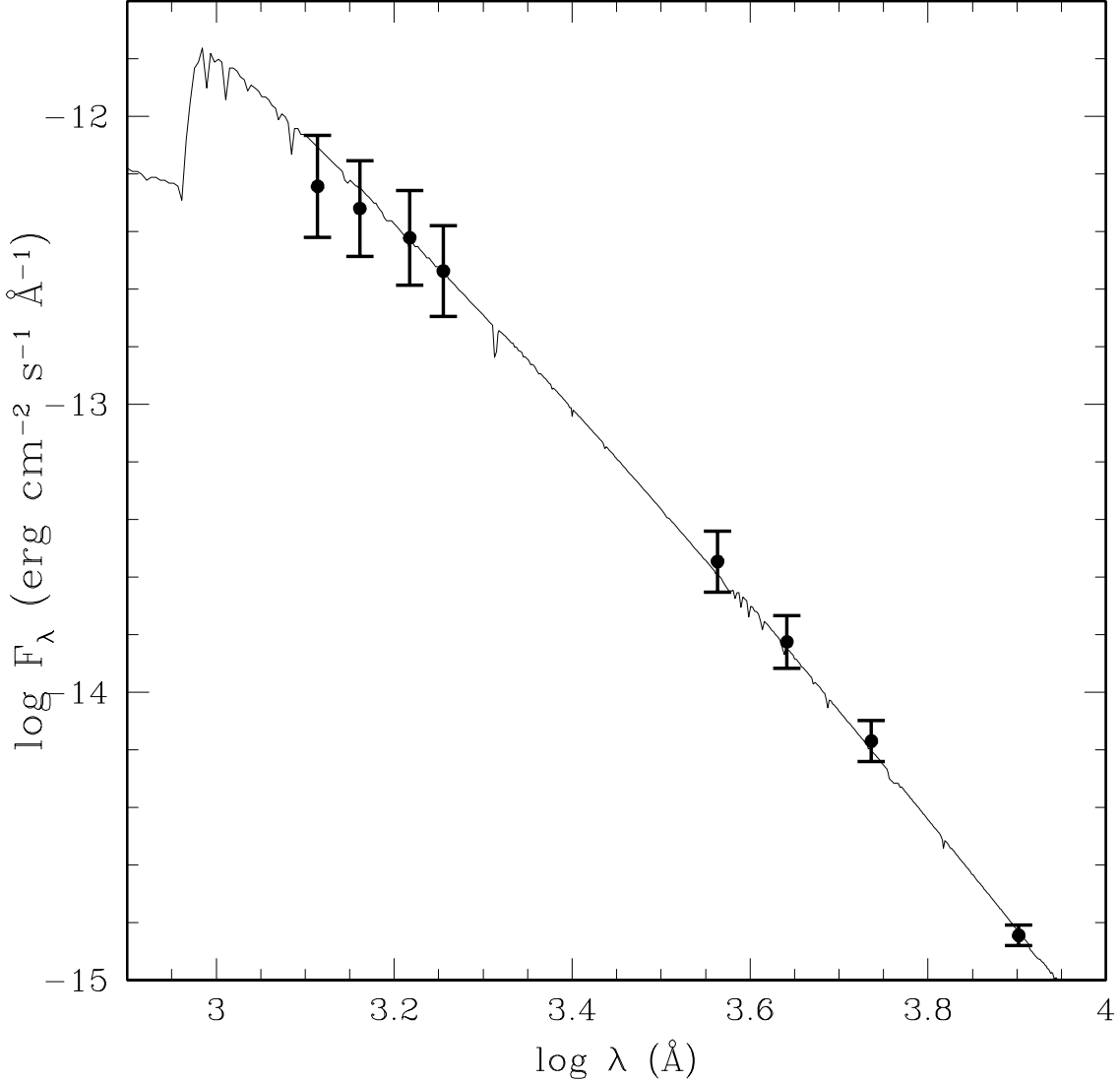


Fig. 1.— Dereddened *HST*/WFPC2 and FOS flux data points for the central star of K 648 are shown with error bars corresponding to  $\pm 0.01$  in  $E(B - V)$ . The error bars illustrate the relative sensitivities of the *HST*/WFPC2 and FOS data to uncertainties in the reddening and the respective weights employed in our SED fitting trials (the optical flux data are given the highest weight). We adopted a foreground reddening of  $E(B - V) = 0.10$ , and found a best-fit total reddening of  $E(B - V) = 0.13$ ; the excess presumably arises from the K 648 nebular material. Overplotted is a model spectrum from Lejeune et al. (1997) for  $[\text{Fe}/\text{H}] = -2.0$ ,  $\log g = 5$ , and  $T_{\text{eff}} = 40,000$  K. The implied luminosity of the K 648 central star is  $\log(L/L_\odot) = 3.78 \pm 0.08$ .

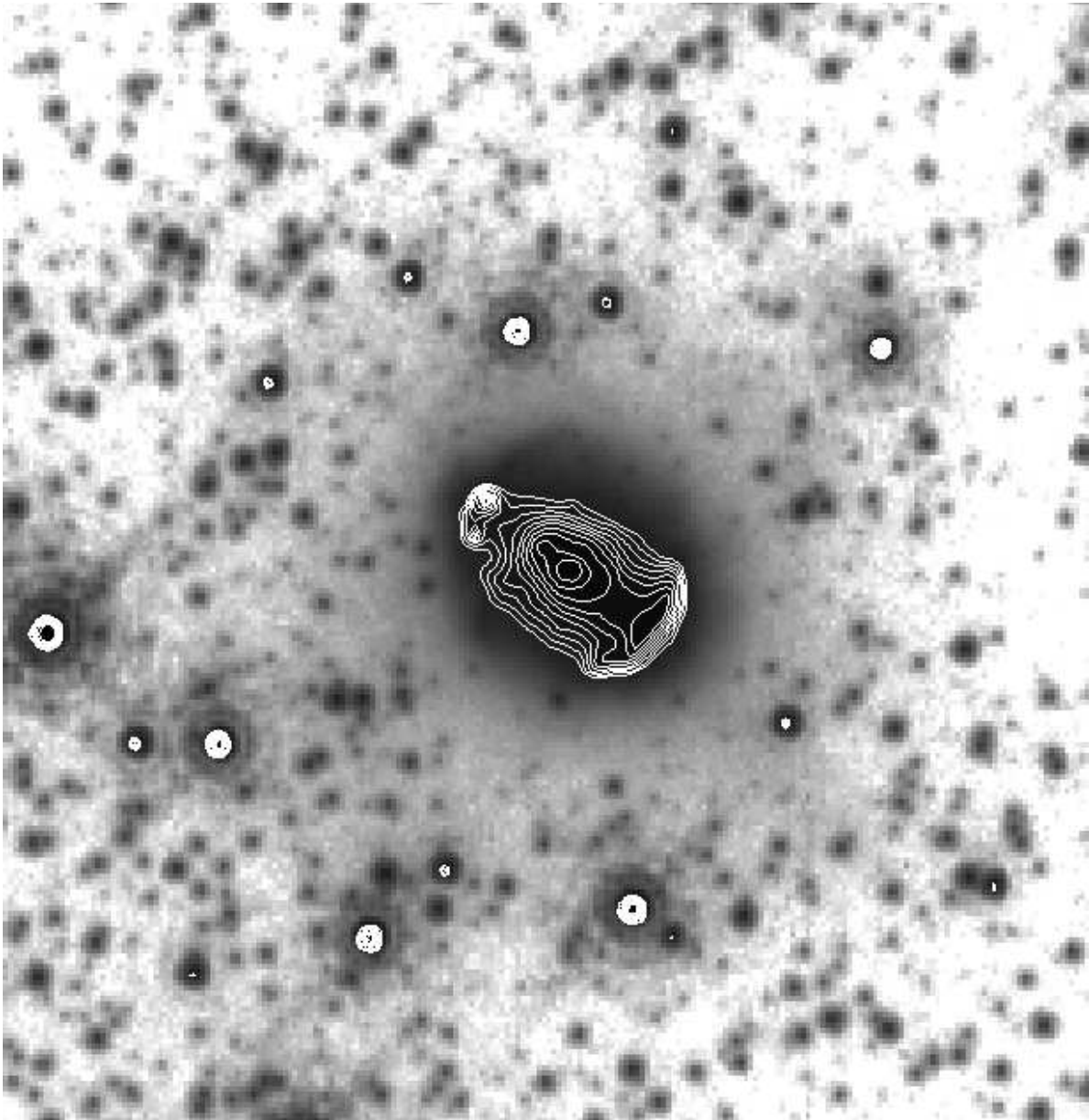


Fig. 2.— Deep WFPC2 image of K 648 in the light of  $H\alpha$ . A logarithmic stretch has been chosen to show the very faint outer halo around K 648, and the overexposed outermost of the nebula’s bright elliptical shells. The inner elliptical shell is shown by superposed isophotes; here the contours are logarithmic, in 10 steps of 0.1 dex. The field of view is  $210\times 210$  pixels, or 8.4 arcsec on a side. North is 11 degrees clockwise from the right, and east is 11 degrees clockwise from straight up.

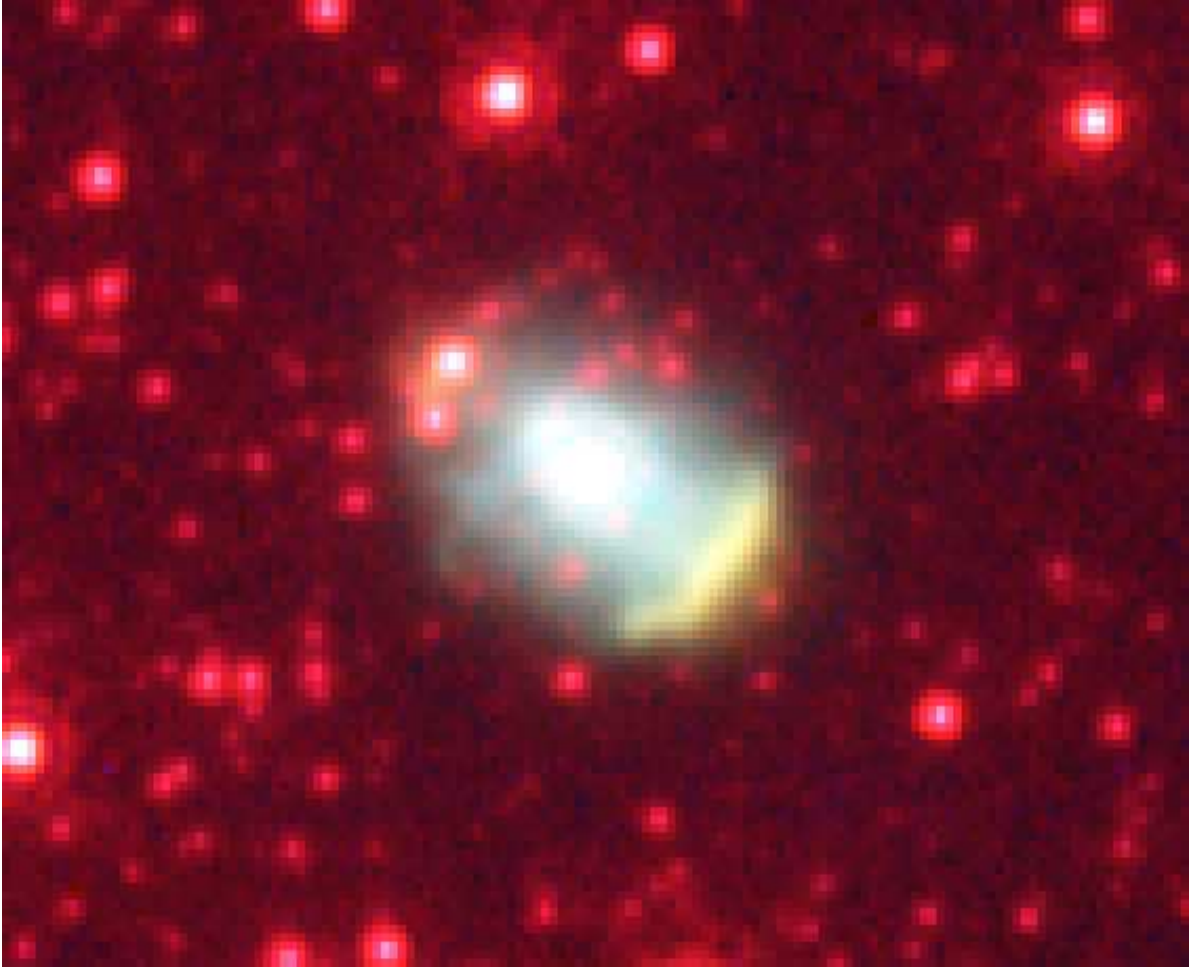


Fig. 3.— False-color WFPC2 image of K 648 in the light of [O III] 5007 Å (blue), H $\alpha$  (green), and [N II] 6583 Å (red). Intensity is log-scaled, and the scale and orientation can be inferred from Fig. 2. This figure illustrates the inner and outer elliptical shells and the bright arc of “FLIERS” on the northwestern edge of the outer elliptical shell. In this representation the large outer halo is too faint to be seen.

Table 1. K 648 Central Star Flux Measurements

$\lambda$ (Å)	Mag. <sup>a</sup>	$F_\lambda$ <sup>b</sup>	$F_\lambda$ IUE <sup>b</sup>	$F_\lambda$ FOS <sup>b</sup>	$A_\lambda/A_V$ <sup>c</sup>	$F_{\lambda,0}$ <sup>b,c</sup>
1300	...	...	$1.60 \times 10^{-13}$	$1.95 \times 10^{-13}$	2.903	$5.71 \times 10^{-13}$
1450	...	...	$1.56 \times 10^{-13}$	$1.76 \times 10^{-13}$	2.703	$4.79 \times 10^{-13}$
1650	...	...	$1.27 \times 10^{-13}$	$1.42 \times 10^{-13}$	2.645	$3.79 \times 10^{-13}$
1800	...	...	$1.10 \times 10^{-13}$	$1.14 \times 10^{-13}$	2.520	$2.90 \times 10^{-13}$
3660	13.55	$1.59 \times 10^{-14}$	...	...	1.569	$2.84 \times 10^{-14}$
4380	14.60	$9.15 \times 10^{-15}$	...	...	1.322	$1.50 \times 10^{-14}$
5450	14.73	$4.66 \times 10^{-15}$	...	...	1.000	$6.76 \times 10^{-15}$
7980	14.93	$1.20 \times 10^{-16}$	...	...	0.479	$1.43 \times 10^{-15}$

<sup>a</sup> Magnitudes are *UBVI* on the Johnson-Kron-Cousins standard system.

<sup>b</sup> Observed and dereddened fluxes in units of  $\text{erg s}^{-1} \text{cm}^{-2} \text{Å}^{-1}$ .

<sup>c</sup>  $A_\lambda/A_V$  from Cardelli, Clayton, & Mathis (1989); assumes  $A_V/E(B - V) = 3.1$ ; dereddened fluxes correspond to  $E(B - V) = 0.13$ .